A Novel Differential Polarization-shift Keying Scheme for Fiber-optic Communication System

A NOVEL DIFFERENTIAL POLARIZATION-SHIFT KEYING SCHEME FOR FIBER-OPTIC COMMUNICATION SYSTEM

BY

ZHENGKAI CHEN, M.Eng.

A THESIS

SUBMITTED TO THE DEPARTMENT OF ELECTRICAL & COMPUTER ENGINEERING

AND THE SCHOOL OF GRADUATE STUDIES

OF MCMASTER UNIVERSITY

IN PARTIAL FULFILMENT OF THE REQUIREMENTS

FOR THE DEGREE OF

MASTER OF APPLIED SCIENCE

Master of Applied Science (2010) McMaster University

(Electrical & Computer Engineering) Hamilton, Ontario, Canada

TITLE:	A Novel Differential Polarization-shift Keying Scheme for Fiber-optic Communication System
AUTHOR:	Zhengkai Chen M.Eng., (Physical Electronics) Graduate University of Chinese Academy of Sciences, Beijing, China
SUPERVISOR:	Dr. Shiva Kumar
NUMBER OF PAGES:	xi, 57

To my Mom, Dad, and Sister

Abstract

The rapid development of fiber-optic communication system requires a increasing transmission data rate and reach. One of the challenge for long-haul high-speed fiber-optic system is how to reduce the impairments and degrading effects from fiber dispersions and nonlinearity. Although the advances of digital signal processor (DSP) make impairment compensation for the coherent systems become possible, the implementation of coherent system is still expensive. Among the direct detection systems, differential phase-shift keying (DPSK) system shows great advantages over other modulation schemes. Although the recent commercial fiber-optic communication systems are based on DPSK, polarization-mode dispersion and fiber nonlinearity are still limiting factors for DPSK systems. In 2004, a differential polarization-phase-shift keying (DPolPSK) system in which information is encoded in both polarization and phase with multi-level direct detection is proposed, and it is found out the DPolPSK system greatly reduces the effect of nonlinear polarization scattering. With the expectation of getting a better nonlinear tolerance than DPSK system, a novel differential polarization-shift keying (DPolSK) system with balanced direct detection receiver is proposed and compared with DPSK system in terms of fiber dispersion and nonlinearity tolerance.

The DPolSK system encodes information in the polarization angle difference between two adjacent symbols. To transmit bit '1' ('0'), the polarization angle of the current symbol is shifted by $\pi/2$ $(-\pi/2)$ with respect to the previous symbol. A balanced detector based on optical delay interferometer and Faraday rotator is used to demodulate the DPolSK signals. Ideally without dispersion and nonlinearity, the DPolSK has the same receiver current level as DPSK system.

Monter-carlo simulations are conducted to evaluate the DPolSK system in the presence of chromatic dispersion (CD), polarization-mode dispersion (PMD), and fiber nonlinearity (FNL). The simulation results show DPolSK system has the same bit-error-rate (BER) and PMD tolerance as DPSK system when fiber nonlinearity is ignored. However, when nonlinearity is taken account in the system, DPolSK shows overall superiority to DPSK system. The reason that DPolSK has higher nonlinear tolerance than DPSK is also explored. The intra-channel four-wave mixing (IFWM) effect on the DPolSK and DPSK systems are investigated and the simulation results show the ghost pulse generation induced by IFWM is suppressed in DPolSK system as compared to DPSK system, leading to higher nonlinear tolerance.

Acknowledgements

First I would like to thank my supervisor, Dr. Shiva Kumar, for his patient instruction and help throughout my study at McMaster University. Dr. Kumar shows his broad range of knowledge and deep understanding as a prestigious professor in fiber-optic communication area. He has very smart and insightful thoughts and ideas which make problem-solving in my research work goes smoothly. In addition, his lecture is very well-organized and he gives us vivid explanation on the questions in a unique funny way. It is a great pleasure to work with Dr. Kumar.

Second, I would like to thank Dr. Xun Li and Dr. Weiping Huang, for their help with my questions and difficulties in my Master's study.

I appreciate the help from my colleagues and friends in the Photonics CAD Lab, we had a good and harmonious time together.

I also want to thank every friend I get know at McMaster University. I had very impressive experience to be with you.

Last but not least, I would like to thank my Mom, Dad, and sister. They give me endless love and caring, and always give me support or comfort when I need.

Notation and abbreviations

ASE Amplified Spontaneous Emission

BER Bit Error Rate

CD Chromatic Dispersion

DGD Differential Group Delay

DPolSK Differential Polarization-shift keying

DPSK Differential Phase-shift keying

FNL Fiber Nonlinearity

FWM Four-wave Mixing

IFWM Intra-channel Four-wave Mixing

IXPM Intra-channel Cross-phase Modulation

NLSE Nonlinear Schrödinger Equation

PMD Polarization-mode Dispersion

PSP Principle State of Polarization

SOP State of polarization

SPM Self-phase Modulation

XPM Cross-phase Modulation

Contents

Abstract iv

Acknowledgements vi

Notation and abbreviations vii

1 Introduction 1

2 Literature Background 7

2.1 Advanced Modulation Formats 7

2.1.1 Direct Detection DPSK System 9

2.2 Fiber-optic Communication Systems Impairments 14

2.2.1 Chromatic Dispersion 15

2.2.2 Polarization Mode Dispersion 17

2.2.3 Fiber Nonlinearity 19

3 DPolSK System Using Direct Detection 22

3.1 DPolSK Encoding 22

3.2 DPolSK Decoding 25

4 Fiber Channel Model **28**

4.1 Polarization Channel Fluctuations 28

4.1.1 Jone's Matrix 29

4.1.2 Polarization Fluctuation Effect on DPolSK System 31

4.1.3 Polarization Controller (PC) 32

4.2 Nonlinear Polarization Effect 34

4.3 PMD Model 35

5 System Setup and Simulation Results **37**

5.1 Optical Fiber Communication System 37

5.1.1 Transmitter 38

5.1.2 Optical Amplifier 39

5.1.3 Optical Filter 40

5.2 Numerical Method 41

5.3 Simulation Results 42

5.3.1 Linear Performance 42

5.3.2 PMD Impairment 43

5.3.3 Fiber Nonlinearity and Dispersion 45

5.3.4 PMD, Dispersion, and PMD 49

6 Conclusions **51**

List of Figures

2.1 Symbol diagrams for (a) OOK and (b) DPSK. The 3-dB sensitivity advantage of DPSK is due to the $\sqrt{2}$-increased symbol spacing for equal average optical power. 11

2.2 Transmitter and direct detection receiver for optical DPSK system . . 12

2.3 Polarization-mode dispersion in optical fiber. $\Delta\tau$: Differential group delay 18

3.1 Symbol set of bit sequence '1011' 24

3.2 Schematic of DPolSK scheme. PBS = Polarization beam splitter. MZM = Mach-zehnder modulator. 25

3.3 Interferometric Direct detection receiver for DPolSK 26

4.1 The received current vs. time. R =1 A/W, amplifier noise is turned off. 33

5.1 Schematic of optical communication system. NDF = Normal dispersion fiber, ADF = Anomalous dispersion fiber, OBF = Optical bandpass filter, PC = Polarization controller. 38

5.2 Linear BER performance of direct detection DPSK and DPolSK, coherent BPSK and PolSK. Transmission distance = 3200 Km 43

5.3 BER vs. DGD for DPolSK and DPSK systems. Transmission distance = 1600 Km and launch power = -8 dBm. Fiber dispersion and nonlinearity are set to zero. (a): 20 runs; (b): 40 runs; (c): 60 runs. . 44

5.4 BER vs. peak launch power for DPSK and DPolSK systems. Transmission distance = 16000 Km. PMD is ignored. 46

5.5 Ghost pulse generation in DPolSK and DPSK systems. Bit sequence '00' is sent, fiber length = 16000 Km, peak launch power = 6 dBm, ASE noise and PMD are turned off. 48

5.6 Ghost pulse generation in DPolSK and DPSK systems. Bit sequence '11' is sent, fiber length = 16000 Km, peak launch power = 6 dBm, ASE noise and PMD are turned off. 49

5.7 BER vs. peak launch power. Transmission distance = 16000 Km, PMD parameter $D_p = 0.05\ ps/\sqrt{Km}$ 50

Chapter 1

Introduction

Fiber-optic communication systems have been deployed worldwide and revolutionized the current and future telecommunication infrastructures. Currently, virtually all the telephone conversations, cell phone calls, high definition television (HDTV), and Internet packets must pass through some pieces of optical fiber from source to destination. While initial deployment of optical fiber was mainly for long-haul or submarine transmission, lightwave systems are currently in virtually all metro networks. Nowadays the deployment of optical fiber is moving toward the home for broadband access. Fiber-to-the-premise (FTTP) and fiber-to-the-home (FTTH) are being considered seriously in most parts of the world right now (Ho, 2005).

Currently most of the commercially available fiber-optic communication systems use the intensity of lightwave to carry information, which is called intensity-modulated/direct detection (IMDD) systems. The IMDD system modulate the signal '1' by sending lightwave pulse of a certain intensity, and '0' by sending no pulse. Photodiode is used to convert the optical signal into electrical current at the receiver so only the intensity

of signal is detected. Both of the transmitter and receiver of IMDD systems are easy to implement and inexpensive. However, the signal quality and receiver sensitivity are poor in IMDD systems.

Actually not only the intensity but also the phase, frequency, and polarization of light can carry information. The corresponding modulation formats are phase-shift keying (PSK), frequency-shift keying (FSK) and polarization-shift keying (PolSK). To detect the information included in the phase or frequency, coherent detection scheme is always required. Coherent systems have higher channel capacity and receiver sensitivity, but they are much more sensitive to lase phase noise, nonlinear phase noise, and polarization variations than OOK systems. The invention of erbium-doped fibre amplifier (EDFA) in the early 1990s has improved the receiver sensitivity for OOK system so the coherent detection became less attractive due to its complexity to realize. However, the coherent communication systems come back recently because the advances in digital signal processor (DSP) make the phase and polarization management become feasible. The DSP based carrier phase estimation algorithm is proposed for laser phase noise and channel additive noise, and is implemented both in simulations and experiments (Dany-Sebastien Ly-Gagnon, 2006), (Kikuchi, 2006), (Goldfarb and Li, 2006). Meanwhile, based on DSP, wireless communication channel estimation algorithm is applied to optical polarization channel and polarization channel matrix can be estimated either by using training sequence (Han and Li, 2005) or blind estimation method (Godard, 1980), (Li, 2009).

However, the coherent system is still expensive to implement and most of the commercial fiber-optic system nowadays are based on the square-law detection. The

differential phase-shift keying (DPSK) system based on direct detection was proposed in 2002 (Gnauck and Gill, 2002). The DPSK system encodes information on the phase difference between two adjacent symbols: to send bit '1', a π phase shift introduced with respect to the previous symbol; whereas a '0' bit is represented by the absence of a phase change. A balanced receiver for DPSK demodulation converts the phase information into intensity information prior to the direct detection. The main advantage of using DPSK instead of OOK comes from a 3-dB receiver sensitivity improvement (Humblet and Azizoglu, 1991). Moreover, both experimental and simulation results show that the Direct-Detection DPSK system has a better tolerance of chromatic dispersion (CD) and polarization-mode dispersion (PMD) than OOK systems (Gnauck and Gill, 2002), (Griffin and Carter, 2002) , (W. Christoph and R.Werner, 2002) , (Wang and Kahn, 2004) , (Chongjin Xie and Hunsche, 2003), (Chris Xu, 2004), (Yutaka Miyamoto, 2002). In phase-modulated optical systems, fiber nonlinearity translates amplitude fluctuations due to amplifier noise into phase fluctuations which is known as nonlinear phased noise or Gordon-Mollenauer noise (Gordon and Mollenauer, 1990). The PMD and especially nonlinear phase noise are the main limitation factors for long-haul high-speed DPSK system (Ho, 2003b), (Kim and Gnauck, 2003).

The optical fiber has two orthogonal polarization channels, and the state of polarization (SOP) of light can be used to represent different symbols. These modulation formats based on SOP are called Polarization-shift keying (PolSK) schemes. PolSK system is sensitive to polarization fluctuations during its propagation, therefore usually a polarization tracking circuit is needed before the receiver. Despite the difficulties in polarization management for PolSK, it has large tolerance to lase phase

noise (Jaume Comellas and Prat, 2004), (S. Benedetto and Poggiolini, 1995).

A differential Polarization-shift keying (DPolSK) system based on coherent detection was proposed (You Imai and James, 1990), (Hou and Wu, 2002) and it has been theoretically and experimentally proved to be immune to phase noise and phase jitter (You Imai and James, 1990), (Benedetto and Poggiolini, 1992). A novel differential polarization-phase-shift keying (DPolPSK) is proposed in which information is encoded in both polarization and phase (Han and Li, 2004). The advantage of this scheme is that the DPolPSK signals are demodulated by the standard DPSK receivers based on optical delayed interference and electrical multilevel detection. The effects of optical nonlinearities on the fiber transmission of DPolPSK are studied and it is found that differential detection greatly reduces the effect of nonlinear polarization scattering. In this thesis, we propose a different type of DPolSK in which information is encoded as a differential polarization state with respect to the previous symbol. To transmit a bit '1' ('0'), the polarization angle of the current symbol is shifted by $\pi/2$ $(-\pi/2)$ with respect to the previous symbol. A novel balanced detector based on optical delay interferometer and Faraday rotator for the demodulation of the DPolSK symbols is also proposed. Although direct detection is used in this paper, the proposed balanced demodulator can be implemented in electrical domain when coherent detection is used.

The remainder of the thesis is organized as follows:

In chapter 2, literature background on advanced modulation formats, linear and nonlinear impairments for the optical fiber communication systems is provided. DPSK systems are discussed in detail for the following reasons: DPSK is the most popularly studied direct detection system in recent years and it shows overall superiority to

OOK system. So the evaluation of our new direct detection DPolSK scheme is based on the comparison with DPSK system. For the linear and nonlinear impairments to optical fiber communication system, we introduce linear impairments such as chromatic dispersion (CD), polarization mode dispersion (PMD), and nonlinear effects such as self-phase modulation (SPM), cross-phase modulation (XPM), and four-wave mixing (FWM). The tolerance of DPolSK/DPSK system to these impairments is an important criteria in the evaluation of these systems.

In chapter 3, transmitter and receiver of the novel DPolSK system are introduced. DPolSK signals are encoded in the polarization angle difference between two neighboring symbols. We introduce a $\pi/2$ polarization angle shift with respect to the previous symbol when bit '1' is sent. Otherwise, to send bit '0', a $-\pi/2$ polarization angle shift with respect to the previous symbol is introduced. A balanced direct detector based on optical delay interferometer and Faraday rotator for the demodulation of the DPolSK symbols is also proposed here. Theoretically, without any impairments and degrading effects, the DPolSK system has the same detected current level as DPSK system.

In Chapter 4, the simulation models for the DPolSK system are discussed and analyzed. The state of polarization (SOP) of light change with time when it propagates in the fiber. Also, the imperfection of fiber introduce birefringence between two principle states of the polarization. These channel fluctuation will affect the DPolSK performance results. To suppress the polarization fluctuation effect on DPolSK system, we introduce a polarization controller (PC) so as to maximize the receiver current. Meanwhile, the simulation models for PMD and fiber nonlinearity in polarization channel are proposed.

In chapter 5, we setup the DPolSK system with fiber parameters and components including amplifier and optical filter. Split-step Fourier method is used to solve the vector nonlinear Schrödinger equation. Then the simulation results are shown for the BER performance comparison of DPolSK and DPSK system in the presence of CD, PMD, and nonlinearity. The DPolSK system is found to have higher nonlinear tolerance than DPSK. The reason for advantage of DPolSK over DPSK is discussed and analyzed. In the case of DPSK, the phases of the neighboring symbols vary, but the polarization angles are roughly the same. However, for DPolSK signals, there is a $\pi/2$ polarization rotation between adjacent symbols and therefore, the phases as well as polarization angles of the neighboring symbols vary and thereby, a better averaging of intra-channel four-wave mixing (IFWM) is achieved.

In chapter 6, we draw the main conclusion of the thesis and possible future work is stated.

Chapter 2

Literature Background

In this chapter, we introduce several advanced modulation formats for optical communication systems. Direct detection DPSK system is discussed in detail because most of our research work on DPolSK are based on evaluation comparison with DPSK system. Meanwhile, linear and nonlinear impairments of different modulation schemes for optical fiber communication systems are discussed in this chapter.

2.1 Advanced Modulation Formats

The electrical field of optical carrier can be expressed as

$$\boldsymbol{E}(t) = \hat{e}Ae^{j\omega t+\phi}. \tag{2.1}$$

In (2.1), the polarization direction $\hat{e}$, the amplitude A, the frequency ω, and the

phase ϕ can be used to carry information. The classification of modulation formats are as follows:

Polarization $\hat{e}$: Polarization-shift keying (PolSK): information is encoded by the state of polarization. For example, bit '1' and '0' are represented by $\hat{e}_x$ and $\hat{e}_y$, respectively; Differential polarization-shift keying (DPolSK): information is encoded by the polarization angle difference between two adjacent symbols. For example, to transmit '1' ('0'), a $\pi/2$ $(-\pi/2)$ polarization rotation is introduced with respect to the previous symbol.

Amplitude A: On-off keying (OOK): information is encoded by the intensity of light. For example, to transmit '1' ('0'), the pulse with amplitude A (0) is used to represent the signal.

Frequency ω: Frequency-shift keying (FSK): information is encoded by the frequency of carrier wave.

Phase ϕ: Phase-shift keying (PSK): information is encoded by the phase of the light. For example, bit '1' and '0' are represented by π and 0, respectively; Differential phase-shift keying (DPSK): information is encoded by the phase difference between two adjacent symbols. For example, to transmit '1' ('0'), a π (0) phase change is introduced with respect to the previous symbol.

The pulse shapes can be classified as non-return to zero (NRZ) and return to zero

(RZ) schemes. NRZ formats take account of the fact that the optical power does not return to zero between two successive '1' bits. The simplest optical modulation format to generate is NRZ-OOK. Because of its simplicity, this is also the most widely deployed format in the optical fiber communication systems. The NRZ OOK system has following merits: First, it requires a relatively low electrical bandwidth for the transmitters and receivers (compared with RZ); Second, it is immune to laser phase noise (compared with PSK); Third, it has the simplest configuration of transceivers.

Like NRZ, RZ can be used in connection with almost any digital modulation format by having the modulation waveform take on a pulse-like shape within the symbol duration. Using RZ waveforms as the basis for a modulation format has important consequences on nonlinear transmission. The signal spectrum is broader than its NRZ equivalent, which generally favors nonlinear transmission, especially at high speeds of 10 Gb/s and above (Winzer and Essiambre, 2008).

2.1.1 Direct Detection DPSK System

Modulation formats in which the data is encoded on the carrier phase are referred to as phase shift keying (PSK) formats. Due to the dominance of square-law detection in optical communications today, the vast majority of phase modulated systems employs differential detection, and the formats are thus referred to as differential phase shift keying (DPSK).

DPSK Transmitter

In DPSK system, information is encoded by the phase difference $\Delta\phi$ between two neighboring symbols. For example, we introduce a π phase change with respect to the previous symbol when bit '1' is sent, while the phase will be left alone when bit '0' is sent. The phase different $\Delta\phi \in \{o, \pi\}$, and the symbol set is $\{e^{j0}, e^{j\pi}\}$ or $\{1, -1\}$. The DPSK transmitter can be composed of precoder, laser and phase modulator, as shown in part (a) of 2.2. The precoder generate drive signal d_k which applies to the phase modulator. We assume the transmitted data is $b_k \in \{0, 1\}$ and the relationship between precoded signal and transmission signal is

$$d_k = d_{k-1} \oplus b_k, \tag{2.2}$$

where d_{k-1} is the previous precoded signal of d_k. The drive signal $d_k \in 0, 1$ applies to phase modulator and generate corresponding signal $-1, 1$.

The main advantage of using DPSK instead of OOK comes from a 3-dB receiver sensitivity improvement, which can be intuitively understood from Figure 2.1, showing that the symbol spacing for DPSk is increased by $\sqrt{2}$ compared to OOK for fixed average optical power (Gnauck and Winzer, 2005). This increased symbol distance makes DPSK accept a $\sqrt{2}$ larger standard deviation of the optical field noise than OOK for the same BER, which translates into a 3-dB reduction in the required optical signal-to-noise ratio (OSNR).

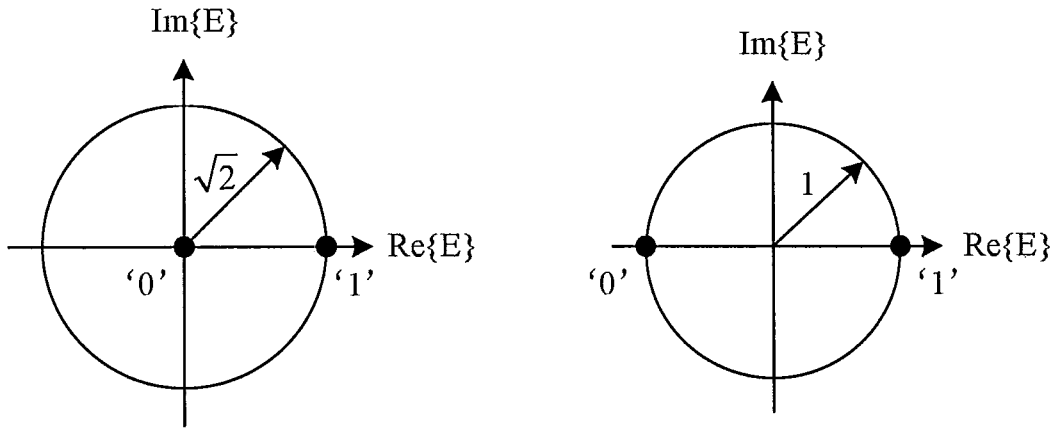

(a) OOK (b) DPSK

Figure 2.1: Symbol diagrams for (a) OOK and (b) DPSK. The 3-dB sensitivity advantage of DPSK is due to the $\sqrt{2}$-increased symbol spacing for equal average optical power.

DPSK Receiver

The demodulation schemes for DPSK system contain coherent detection and direct detection. Interferometric direct detection scheme for DPSK is shown in Figure 2.2, which is much easier to implemented than the coherent detection with a local oscillator (LO) laser for DPSK system. The optical signal is split into two paths and then combined after a path difference of an one-bit period delay T, and a π phase shift is introduced at one of the path signal. Two photodiodes (PD) convert the optical signals into electrical currents (suppose the responsivity of the PD is 1). The mathematical form of the demodulation for direct detection DPSK is interpreted as

$$I = \|\boldsymbol{E}_s(t) + \boldsymbol{E}_s(t - T_b)\|^2 - \|\boldsymbol{E}_s(t) - \boldsymbol{E}_s(t - T_b)\|^2 . \tag{2.3}$$

Suppose the initial symbol is aligned with x-axis, then it can be represented by a

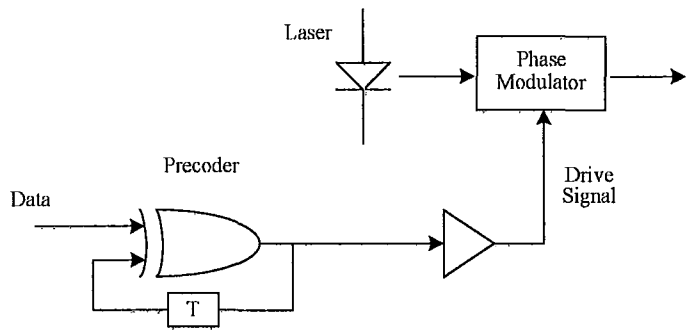

(a) DPSK transmitter

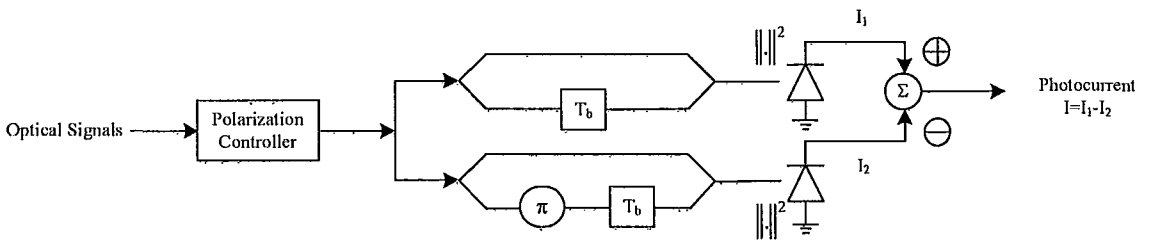

(b) Direct detection DPSK receiver

Figure 2.2: Transmitter and direct detection receiver for optical DPSK system

vector as:

$$\begin{bmatrix} A \\ 0 \end{bmatrix}, \tag{2.4}$$

where the upper and lower rows correspond to x- and y- polarization components. To send bit '1', a π phase shift is introduced with respect to the initial symbol, then the second symbol can be expressed as:

$$\begin{bmatrix} -A \\ 0 \end{bmatrix}. \tag{2.5}$$

In the following, we send a bit '0', then the phase is left alone with respect to the second symbol, so the third symbol is represented as:

$$\begin{bmatrix} -A \\ 0 \end{bmatrix}. \tag{2.6}$$

Therefore, to send bit sequence of '10', the symbol sequence is

$$\begin{bmatrix} A \\ 0 \end{bmatrix} \begin{bmatrix} -A \\ 0 \end{bmatrix} \begin{bmatrix} -A \\ 0 \end{bmatrix}. \tag{2.7}$$

Suppose bit '1' is transmitted with

$$\boldsymbol{E}_s(t - T_b) = \begin{bmatrix} A \\ 0 \end{bmatrix}, \tag{2.8}$$

and

$$\boldsymbol{E}_s(t) = \begin{bmatrix} -A \\ 0 \end{bmatrix}, \tag{2.9}$$

the demodulation formula (2.3) becomes

$$I = 4A^2. \tag{2.10}$$

Similarly, Suppose bit '0' is transmitted with

$$\boldsymbol{E}_s(t - T_b) = \begin{bmatrix} -A \\ 0 \end{bmatrix}, \tag{2.11}$$

and

$$\boldsymbol{E}_s(t) = \begin{bmatrix} -A \\ 0 \end{bmatrix}, \tag{2.12}$$

the demodulation formula (2.3) becomes

$$I = -4A^2. \tag{2.13}$$

So in the direct detection DPSK system, the received currents for bit '1' and '0' are $4A^2$ and $-4A^2$, respectively.

2.2 Fiber-optic Communication Systems Impairments

In an optical fiber communication system, linear impairments include fiber loss, chromatic dispersion (CD) and polarization mode dispersion (PMD). Optical power loss due to attenuation can be compensated easily by an optical amplifier. CD and PMD are the main linear impairments for the optical communication systems. Nonlinear degrading effects induced by fiber nonlinearity are self-phase modulation (SPM), cross-phase modulation (XPM), four-wave mixing (FWM), stimulated Raman scattering (SRS) and stimulated Brillouin scattering (SBS).

The signal propagation over optical fibers in single mode condition is described as nonlinear Schrödinger equation (NLSE), which describes the evolution of optical waveform at the transmission distance z is given by

$$\frac{\partial A}{\partial z}+\frac{\alpha}{2}A+\frac{i}{2}\beta_2\frac{\partial^2 A}{\partial T^2}-\frac{1}{6}\beta_3\frac{\partial^3 A}{\partial T^3}=i\gamma\left[|A|^2A+\frac{i}{\omega_0}\frac{\partial}{\partial T}(|A|^2A)-T_RA\frac{\partial|A|^2A}{\partial T}\right], \quad (2.14)$$

where T is time in the frame of reference moving with the pulse at the group velocity V_g and $T = t - z/V_g = t - \beta_1 z$; $|A|^2$ represents optical power, γ is the nonlinearity coefficient, α is the attenuation constant, β_1, β_2 and β_3 are the first order, second order and third order derivative of mode-propagation constant β about the center frequency ω_0, and T_R is related to the slope of the Raman gain and is usually estimated to be ~ 5 fs. The term which is proportional to β_3 accounts for the higher order of dispersion which becomes important for ultra-short pulses. The last two terms in the right side of the equation are related to the effects of self-steepening and stimulated Raman scattering, respectively.

2.2.1 Chromatic Dispersion

The fundamental mechanism of chromatic dispersion is the frequency dependence of the refractive index $n(\omega)$. Because the velocity of light is determined by $c/n(\omega)$, the different spectral components associated with the pulse would travel at different speeds. The dispersion-induced spectrum broadening would be very important even without nonlinearity. The effects of dispersion can be accounted for by expanding the mode-propagation constant β in a Tayler series about the center frequency ω_0:

$$\beta(\omega) = n(\omega)\frac{\omega}{c} = \beta_0 + \beta_1(\omega - \omega_0) + \frac{1}{2}\beta_2(\omega - \omega_0)^2 + \cdots, \tag{2.15}$$

where

$$\beta_m = \left[\frac{d^m\beta}{d\omega^m}\right]_{\omega=\omega_0} (m = 0, 1, 2, \cdots). \tag{2.16}$$

So it is easy to get the first and second order derivatives from Eqs. 2.15 and 2.16:

$$\beta_1 = \frac{1}{c}\left[n + \omega\frac{dn}{d\omega}\right] = \frac{1}{V_g}, \tag{2.17}$$

$$\beta_2 = \frac{1}{c}\left[2\frac{dn}{d\omega} + \omega\frac{d^2n}{d\omega^2}\right] \approx \frac{\lambda^3}{2\pi c^2}\frac{d^2n}{d\lambda^2}, \tag{2.18}$$

where c is the speed of light in vacuum. λ is the wavelength.

The wavalength where $\beta_2 = 0$ is called zero-dispersion wavelength λ_D. However, there is still dispersion at wavelength λ_D and higher order dispersion will be considered in this case. Another parameter concerning the dispersion of fiber is more often used, which is often referred to as a dispersion parameter D. The relationship between D and β_1, β_2 is shown as following:

$$D = \frac{d\beta_1}{d\lambda} = -\frac{2\pi c}{\lambda^2}\beta_2 \approx -\frac{\lambda}{c}\frac{d^2n}{d\lambda^2}. \tag{2.19}$$

From (2.19), we can see that D has opposite sign with β_2. When $\lambda < \lambda_D$, $\beta_2 > 0$ (or $D < 0$), the fiber is said to exhibit normal dispersion. In the normal-disperison regime, high-frequency components of optical signal travel slower than low-frequency components. On the contrary, in the regime where wavelength $\lambda > \lambda_D$, $\beta_2 < 0$ (or $D > 0$), fiber is said to exhibit anomalous-dispersion. In the anomalous-dispersion regime, high-frequency components of signal travel faster than low-frequency components.

Dispersion plays an important role in signal transmission over fibers. The interaction between dispersion and nonlinearity is an important issue in lightwave system design.

2.2.2 Polarization Mode Dispersion

The light speed along with two principles state of polarization (PSP) are the same if the profile of optical fiber is ideally circular. But actually due to manufacture variance, the profile of optical fiber deviates slightly from being circular. The light speeds along two PSPs are slightly different and therefore, the signals transmitted along two axis do not arrive at the fiber terminal simultaneously, as we can see in Figure 2.3. This phenomenon is called polarization-mode dispersion (PMD). The first-order of PMD is represented by differential group delay (DGD), which is the time offset when signals transmitting along two PSPs arrive at the receiver. The DGD is a radom variable and has a Maxwellian distribution of

$$p(\Delta\tau) = \frac{32\Delta\tau^2}{\pi^2\langle\Delta\tau\rangle^3} exp\left(-\frac{4\Delta\tau^2}{\pi\langle\Delta\tau\rangle^2}\right), \Delta\tau > 0, \tag{2.20}$$

with a DGD second-order moment of $E\{\Delta\tau^2\} = 3\pi\langle\Delta\tau\rangle^2/8$. For a long optical fiber, all statistical PMD properties of the fiber depend only on the mean DGD $\langle\Delta\tau\rangle$. The

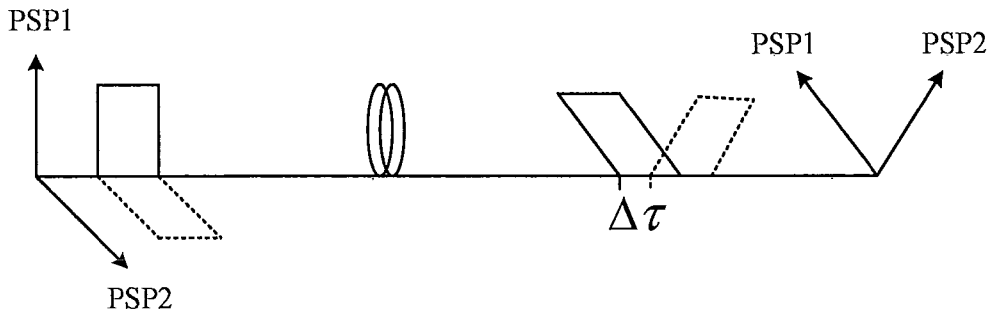

Figure 2.3: Polarization-mode dispersion in optical fiber. $\Delta\tau$: Differential group delay

mean DGD $\langle\Delta\tau\rangle$ is proportional to $\sqrt{L}$, where L is the fiber length. And we have the following expression for $\langle\Delta\tau\rangle$ as

$$\langle\Delta\tau\rangle = D_p\sqrt{L}, \tag{2.21}$$

where D_p is called PMD coefficient. Currently, the PMD coefficient value is around 0.1 $ps/\sqrt{km}$, in some commercial optical fiber system, the D_p value can be approaching 0.05 $ps/\sqrt{km}$.

The PSPs fluctuate with time when signal transmits through fiber, as we have demonstrated in the previous section. We can see from Figure 2.3 the two PSPs are different from their original directions besides the two orthogonal polarized components have DGD at the fiber terminal. In our PMD simulation model (see chapter 4), we have taken both PSP fluctuations and DGD variations into consideration.

2.2.3 Fiber Nonlinearity

Self-phase Modulation and Cross-phase Modulation

Self-phase modulation (SPM) and cross-phase modulation (XPM) are the two most important nonlinear effects which originate from the intensity dependence of the refractive index. SPM refers to the self-induced power-dependent phase shift experienced by an optical field during its propagation in optical fibers.XPM refers to the nonlinear phase shift of an optical field induced by a co-propagating field at a different wavelength.

When two optical fields at frequencies ω_1 and ω_2, polarized along the x axis, co-propagate simultaneously inside the fiber, the optical field can be written as:

$$E = \frac{1}{2}\hat{x}[E_1 exp(-i\omega_1 t) + E_2 exp(-i\omega_2 t) + c.c.]. \tag{2.22}$$

Nonlinear phase shift for the field at ω_1 induced by SPM and XPM can be expressed as:

$$\phi_{NL} = n_2 k_0 L(|E_1|^2 + 2|E_2|^2), \tag{2.23}$$

where n_2 is the nonlinear-index coefficient, $k_0 = 2\pi/\lambda$ and L is the fiber length. On the right-hand side of (2.23), the first term $n_2 k_0 L|E_1|^2$ is the SPM-induced nonlinear phase shift; the second term $2n_2 k_0 L|E_2|^2$ is the XPM-induced nonlinear phase shift. So for equally intense optical fields, the contribution of XPM to the nonlinear phase shift is twice compared with that of SPM.

Intra-channel Nonlinear Effects

Basically, the NLSE (2.14) can be simplified as

$$\frac{\partial A}{\partial z} + \frac{\alpha}{2}A + \frac{i}{2}\beta_2\frac{\partial^2 A}{\partial T^2} = i\gamma|A|^2 A. \tag{2.24}$$

The nonlinear term $i\gamma|A|^2A$ is caused by Kerr nonlinear effect. Assuming a solution of the form $A = A_0 + \Delta A$ in (2.24), where A_0 is the solution of the linear equation and ΔA is the perturbation induced in the linear solution due to the Kerr effect, we obtain the following equation for the nonlinear perturbation:

$$\frac{\partial \Delta A}{\partial z} + \frac{\alpha}{2}\cdot\Delta A + \frac{i}{2}\beta_2\frac{\partial^2 \Delta A}{\partial T^2} = i\gamma|A_0 + \Delta A|^2(A_0 + \Delta A). \tag{2.25}$$

Assuming that the perturbation term is very small in comparison with the linear one, for the perturbation ΔA we can obtain the following linear equation

$$\frac{\partial \Delta A}{\partial z} + \frac{\alpha}{2}\cdot\Delta A + \frac{i}{2}\beta_2\frac{\partial^2 \Delta A}{\partial T^2} = i\gamma|A_0|^2 A_0. \tag{2.26}$$

If we consider the propagation of two pulses A_1 and A_2, we have $A_0 = A_1 + A_2$ and we have

$$\begin{aligned}\frac{\partial \Delta A}{\partial z} + \frac{\alpha}{2}\cdot\Delta A + \frac{i}{2}\beta_2\frac{\partial^2 \Delta A}{\partial T^2} &= i\gamma\{|A_1|^2A_1 + |A_2|^2A_2\} \\ &+ i\gamma\{2|A_2|^2A_1 + 2|A_1|^2A_2\} \\ &+ i\gamma\{A_1A_2{}^*A_1 + A_2A_1{}^*A_2\}.\end{aligned} \tag{2.27}$$

The first two terms in the right side of (2.27) represent the SPM, the second two terms are responsible for the intra-channel cross phase modulation (IXPM) and the last two terms represent the intra-channel four-wave mixing (IFWM). Because

of IFWM, ghost pulses are generated on either side of the signal pulses A_1 and A_2. If there is a signal pulse at the location of the ghost pulse, it leads to performance degradations.

It is also important to point out that in systems, where the pulses remain in its time slot during the propagation $A_1 \cdot A_2 \approx 0$, which means that the terms related with IXPM and IFWM vanish. But when the pulses have strong broadening due to chromatic dispersion, the IXPM induces timing jitter and the main limiting factors for this regime of transmission are amplitude fluctuations and ghost pulse generation caused by IFWM (Mamyshev and Mamysheva, 1999) (R. J. Essiambre and Raybon, 1999).

Chapter 3

DPolSK System Using Direct Detection

In this chapter, we discuss the DPolSK transmitter and receiver. Full numerical simulation of DPolSK systems with this type of transceiver is carried out in chapter 5.

3.1 DPolSK Encoding

DPolSK format is encoded in the polarization angle difference $\Delta\theta$ between two neighboring symbols. In this thesis, we introduce a clockwise polarization rotation by $\pi/2$ with respect to previous symbol when bit '1' is sent, while a counterclockwise rotation by $\pi/2$ is introduced for bit '0'.

Let us introduce a vector

$$\boldsymbol{E}_i = \begin{bmatrix} E_x \\ E_y \end{bmatrix}, \tag{3.1}$$

to denote the optical field envelope. Where E_i represents the ith signal envelope. Suppose the initial symbol is aligned with x-axis, then we have

$$\boldsymbol{E}_1 = \begin{bmatrix} A \\ 0 \end{bmatrix}. \tag{3.2}$$

Suppose we want to transmit bit '1'. We rotate the polarization of $\boldsymbol{E}_1$ by $\pi/2$. The rotation by an angle θ is represented by a matrix

$$\boldsymbol{M}_\theta = \begin{bmatrix} cos\theta & sin\theta \\ -sin\theta & cos\theta \end{bmatrix}. \tag{3.3}$$

The field envelope of the next symbol is

$$\boldsymbol{E}_2 = \boldsymbol{M}_{\pi/2}\boldsymbol{E}_1 = \begin{bmatrix} 0 \\ -A \end{bmatrix}. \tag{3.4}$$

Suppose the next symbol to be transmitted is bit '0'. We rotate the polarization of $\boldsymbol{E}_2$ by $-\pi/2$. The field envelope of the next symbol is

$$\boldsymbol{E}_3 = \boldsymbol{M}_{-\pi/2}\boldsymbol{E}_2 = \begin{bmatrix} A \\ 0 \end{bmatrix}. \tag{3.5}$$

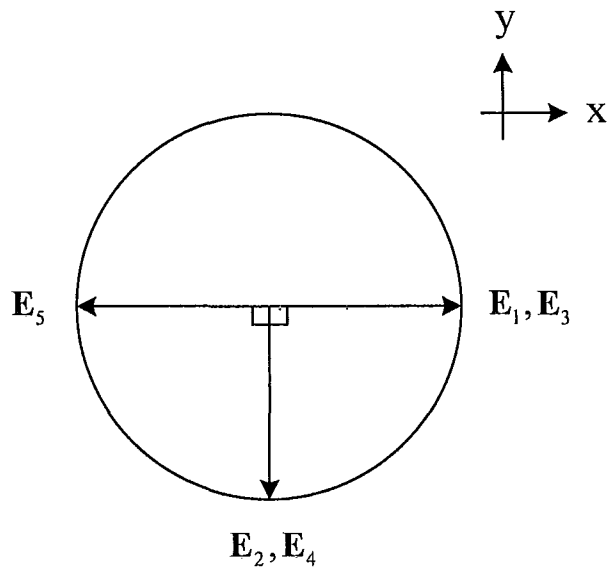

Figure 3.1: Symbol set of bit sequence '1011'

When a bit sequence '1011' is sent, the sequence of vector field envelopes is

$$\begin{bmatrix} A \\ 0 \end{bmatrix} \begin{bmatrix} 0 \\ -A \end{bmatrix} \begin{bmatrix} A \\ 0 \end{bmatrix} \begin{bmatrix} 0 \\ -A \end{bmatrix} \begin{bmatrix} -A \\ 0 \end{bmatrix}. \tag{3.6}$$

Figure 3.1 shows the process of differential polarization shift keying for bit sequence '1011'.

DPolSK scheme can be implemented using two Mach-zehnder modulator (MZM), as shown in Figure 3.2. The laser output is split into two polarization components using polarization beam splitter (PBS). The MZM1 and MZM2 are driven by the outputs of DPolSK encoder1 and DPolSK encoder2 respectively. For example, to obtain the upper row of the (3.6), MZM1 is biased such that its output is three valued 0, A, and $-A$, which is similar to the case of duo-binary modulation format (Winzer and Essiambre, 2006). The output signals of MZM1 and MZM2 are combined using

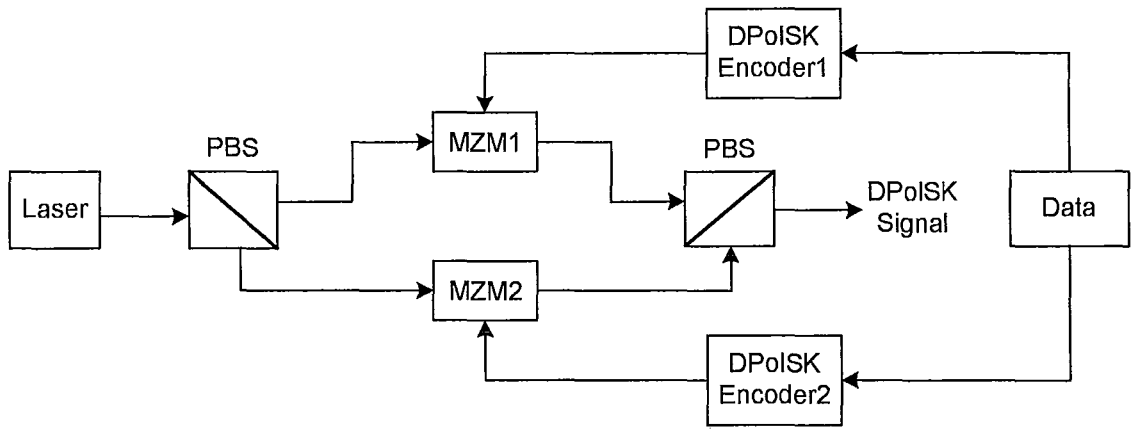

Figure 3.2: Schematic of DPolSK scheme. PBS = Polarization beam splitter. MZM = Mach-zehnder modulator.

PBS to obtain the DPolSK signal.

3.2 DPolSK Decoding

Figure 3.3 shows the balanced direct detection scheme for DPolSK system. At the optical receiver, the input signal is split into two branches. For branch 1, we split the signals into two paths. A Faraday rotator is used to rotate the polarization angle of signal by $\pi/2$ and then delay the signal by one bit period T_b . The other path of signal is kept unchanged. The signals in two paths are combined and a Photodetector convert the optical signals into electrical current I_1 as

$$I_1 = R\|\boldsymbol{E}_s(t) + \boldsymbol{M}_{\pi/2}\boldsymbol{E}_s(t - T_b)\|^2, \tag{3.7}$$

where R is the responsivity of the photodiode, and $\boldsymbol{E}_{\pi/2}$ is the rotational matrix corresponding to Faraday $\pi/2$ rotator. Similarly, for the second branch, we have the

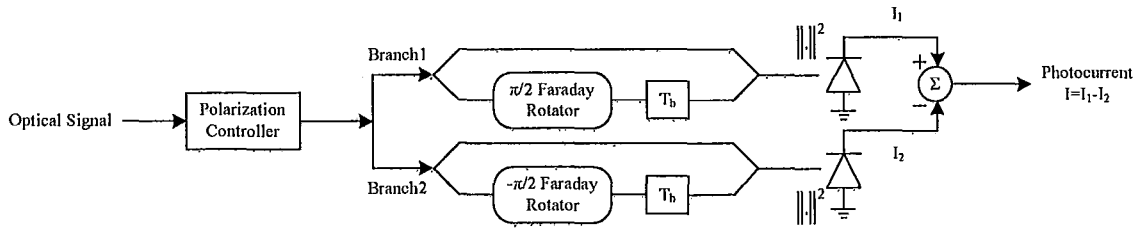

Figure 3.3: Interferometric Direct detection receiver for DPolSK

electrical current I_2 as

$$I_1 = R\|\boldsymbol{E}_s(t) + \boldsymbol{M}_{-\pi/2}\boldsymbol{E}_s(t - T_b)\|^2. \tag{3.8}$$

The final output current I is given by

$$I = I_1 - I_2. \tag{3.9}$$

Suppose bit '1' is tansmitted with

$$\boldsymbol{E}_s(t - T_b) = \begin{bmatrix} A \\ 0 \end{bmatrix}, \tag{3.10}$$

and

$$\boldsymbol{E}_s(t) = \begin{bmatrix} 0 \\ -A \end{bmatrix}. \tag{3.11}$$

Now Eqs. (3.7) (3.8) (3.9) become

$$I_1 = 4A^2R, \tag{3.12}$$

$$I_2 = 0, \tag{3.13}$$

$$I = 4A^2R. \tag{3.14}$$

Similarly, when bit '0' is transmitted, Eqs. (3.7) (3.8) (3.9) become

$$I_1 = 0, \tag{3.15}$$

$$I_2 = 4A^2R, \tag{3.16}$$

$$I = -4A^2R. \tag{3.17}$$

Thus, if the received current I is positive (negative), it would be decided that bit '1' (bit '0') is transmitted. These current values for bit '0' and '1' are the same as that for direct detection DPSK system which encodes initial signal with A and $-A$ (Wang and Kahn, 2004). Although we have considered interferometric demodulation and direct detection, the proposed demodulation technique can be implemented on a digital signal processor (DSP) when coherent detection is employed.

Chapter 4

Fiber Channel Model

Because the states of polarization (SOP) aligned with X-axis and Y-axis are used to carry information in DPolSK system, our system simulation is built based on a vector polarization channel. The SOP of light is not preserved during its propagation in fiber, actually the SOP changes on a timescale ranging from millisecond to month due to environment and situation variations (Misha Boroditsky and Mecozzi, 2005). In this chapter, we will study how the polarization fluctuation affect DPolSK system and introduce a polarization controller (PC) to minimize the polarization effect on the system. PMD, as a linear polarization effect, becomes a challenge for the system when the optical transmission data rate is over 10 Gb/s. We will discuss our PMD simulation model as well as nonlinear effect model in this chapter.

4.1 Polarization Channel Fluctuations

A single-mode optical fiber can support two polarization modes, these two polarization modes are used for polarization-division multiplexing (PDM) or polarization-shift keying (PolSK). If the core of a single-mode fiber is perfectly circular, the two polarization modes propagate with the same speed. However, due to manufacturing tolerance, the core of the fiber varies slightly from perfect circle. The propagation speeds of the two polarization modes have small difference, leading to polarization-mode dispersion (PMD). The optical signal transmitted through the two polarizations arrives with a timing offset at the receiver, called differential group delay (DGD). Even if the fiber is perfectly circular, external mechanical or thermal stresses cause small asymmetric to the fiber core. The DGD changes with time due to external stress.

A long optical fiber can model as the cascade of many pieces of polarized components, each polarized component corresponds to a short piece of fiber with a length about the birefringence correlation length. The two principle states of polarization (PSP) of optical fiber are randomly oriented and the DGD is a random variable, depending on the alignment of individual polarized fiber pieces. Time varying external stress changes both the PSP and DGD.

4.1.1 Jone's Matrix

Let β_x and β_y be the group speeds corresponding to x- and y- polarization. After going through a fiber with length l, the optical field becomes

$$E_{ox} = E_{ix}\, e^{j\beta_{1x}l} \tag{4.1}$$

$$E_{oy} = E_{iy}\, e^{j\beta_{1y}l}, \tag{4.2}$$

where $E_i(x)$ and $E_i(y)$ are the X- and Y- optical field component of input signal. We let

$$\varphi = \frac{(\beta_{1x}l - \beta_{1y}l)}{2} \tag{4.3}$$

$$\Delta = \frac{(\beta_{1x}l + \beta_{1y}l)}{2}, \tag{4.4}$$

where Δ is the common phase and φ is the differential phase. The birefringence effect can be expressed in the matrix form as

$$\begin{bmatrix} E_{ox} \\ E_{oy} \end{bmatrix} = \begin{bmatrix} e^{j(\Delta+\varphi)} & 0 \\ 0 & e^{j(\Delta-\varphi)} \end{bmatrix} \begin{bmatrix} E_{ix} \\ E_{iy} \end{bmatrix} \tag{4.5}$$

The random polarization angle rotation in the fiber can be also expressed in the matrix form of

$$\begin{bmatrix} \cos\theta & -\sin\theta \\ \sin\theta & \cos\theta \end{bmatrix} \tag{4.6}$$

So the signal affected by channel variation with both polarization random rotation and birefringence is depicted as

$$\begin{bmatrix} E_{ox} \\ E_{oy} \end{bmatrix} = \begin{bmatrix} \cos\theta & -\sin\theta \\ \sin\theta & \cos\theta \end{bmatrix} \begin{bmatrix} e^{j(\Delta+\varphi)} & 0 \\ 0 & e^{j(\Delta-\varphi)} \end{bmatrix} \begin{bmatrix} E_{ix} \\ E_{iy} \end{bmatrix} \tag{4.7}$$

To simplify further, we can rewrite (4.7) as

$$\begin{bmatrix} E_{ox} \\ E_{oy} \end{bmatrix} = e^{j\Delta} \begin{bmatrix} \cos\theta\ e^{j\varphi} & -\sin\theta\ e^{-j\varphi} \\ \sin\theta\ e^{j\varphi} & \cos\theta\ e^{-j\varphi} \end{bmatrix} \begin{bmatrix} E_{ix} \\ E_{iy} \end{bmatrix} \tag{4.8}$$

The fator $e^{j\Delta}$ is the common phase of two orthogonal polarization signal components and we can discard it in the following discussion. So we get the matrix to depict polarization channel variations as

$$\begin{bmatrix} \cos\theta\ e^{j\varphi} & -\sin\theta\ e^{-j\varphi} \\ \sin\theta\ e^{j\varphi} & \cos\theta\ e^{-j\varphi} \end{bmatrix}. \tag{4.9}$$

This matrix is called Jone's Matrix. (4.9) is a unitary matrix.

A long optical fiber can model as the cascade of many segments of polarized components, polarization fluctuation effect for each segment is represented by (4.9). Because the multiplication of unitary matrix is still unitary matrix, so after going through a long distance of fiber the channel matrix is composed of multiplication of (4.9) with different θ and φ. The channel matrix can be expressed as follows

$$\boldsymbol{J} = \begin{bmatrix} J_1 & J_2 \\ -J_2^* & J_1^* \end{bmatrix}, \tag{4.10}$$

where J_1 and J_2 are complex numbers which satisfy

$$|J_1|^2 + |J_2|^2 = 1. \tag{4.11}$$

4.1.2 Polarization Fluctuation Effect on DPolSK System

Taking the polarization fluctuation effect into consideration for DPolSK system,

the channel fluctuation matrix (4.10) is applied to signals and the demodulated current in (3.9) is rewritten as

$$I = \left\| \boldsymbol{J}\boldsymbol{E}_s(t) + \boldsymbol{J}\boldsymbol{M}_{\pi/2}\boldsymbol{E}_s(t-T_b) \right\|^2 - \left\| \boldsymbol{J}\boldsymbol{E}_s(t) + \boldsymbol{J}\boldsymbol{M}_{-\pi/2}\boldsymbol{E}_s(t-T_b) \right\|^2. \quad (4.12)$$

Now Eqs. (3.14) and (3.17) are modified as

$$I^{(1)} = 4A^2\kappa R, \text{ when bit '1' is sent} \quad (4.13)$$

$$I^{(0)} = -4A^2\kappa R, \text{ when bit '1' is sent} \quad (4.14)$$

where

$$\kappa = Re(J_1^2 + J_2^2). \quad (4.15)$$

κ is a real number and we can get $|\kappa \leq 1|$ according to (4.11). κ can be positive or negative so it may affect the sign of the detected current. Because the polarization channel drift rate is much slower than the transmission data rate, we can estimate and compensate κ by sending training sequence in the preamble of frame (Li, 2009).

4.1.3 Polarization Controller (PC)

Compensation for the channel effects can be done either in optical or electrical domain. In this thesis, we consider a simple compensation using a polarization controller

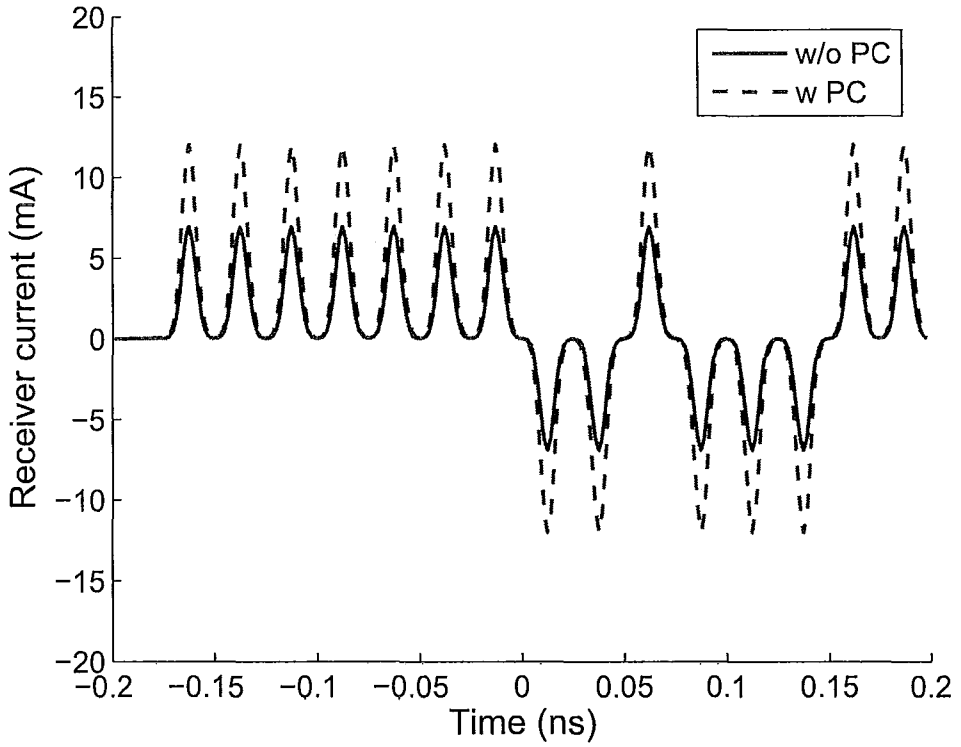

Figure 4.1: The received current vs. time. R =1 A/W, amplifier noise is turned off.

(PC) which can be represented by a matrix

$$M_{PC} = \begin{bmatrix} cos\theta & sin\theta e^{j\varphi} \\ -sin\theta e^{-j\varphi} & cos\theta \end{bmatrix}. \tag{4.16}$$

The angle θ and φ can be adjusted so as to maximize the received current. Because unitary matrix (4.10) does not change the total power of signal and noise, our algorithm to use PC is make the absolute value of κ close to 1 when θ and φ are properly adjusted.

Figure 4.1 shows a case of DPolSK signals dealing with PC. We send 16 bits signal pulse with peak launch power of 3 mw to the fiber-optic system, from (3.9) the ideal

received current should be 12 mA (Assuming R=1 A/W). However, we see from figure 4.1 that the peak current is only 7 mA because of the polarization rotation caused by the fiber-optic channel . In this case the channel matrix $\boldsymbol{J}$ is

$$\begin{bmatrix} 0.710623 - 0.042866i & 0.532433 + 0.457923i \\ -0.532433 + 0.457923i & 0.710623 + 0.042866i \end{bmatrix}, \tag{4.17}$$

and according to (4.15), we can calculate the κ value for our system without PC is 0.5769, which correspond to the peak power 6.923 mA of the solid line without PC in 4.1. In our simulations we change θ of PC from 0 to 2π and φ from 0 to π, both with 500 steps, and find out the rotation matrix $\boldsymbol{M_{PC}}$ which maximize the receiver current, is:

$$\boldsymbol{M_{PC}} = \begin{bmatrix} 0.661312 & -0.592704 - 0.459748i \\ 0.592704 - 0.459748i & 0.661312 \end{bmatrix} \tag{4.18}$$

and after PC our total channel matrix becomes

$$\begin{bmatrix} 0.996048 - 0.001721i & -0.088792 + 0.001529i \\ 0.088792 + 0.001529i & 0.996048 + 0.001721i \end{bmatrix}, \tag{4.19}$$

now the κ value for our system channel is 0.9999, which make our power peak of receiver current get back to the original level, as we can seen from figure 4.1.

4.2 Nonlinear Polarization Effect

The wave propagation equation in optical fiber is usually depicted as Nonlinear Schrödinger Equation (NLSE) as

$$\frac{\partial A}{\partial z} + j\beta_2 \frac{\partial^2 A}{\partial t^2} + \frac{\alpha}{2} A = j\gamma |A|^2 A \tag{4.20}$$

where A is slow-varying envelope, $\beta_2 = -\frac{D(\lambda)\lambda^2}{2\pi c}$, $D(\lambda)$ is the fiber CD parameter, α is fiber loss, and γ is nonlinear parameter. The NLSE is only true for optical fiber transmission system when the polarization state of the carrier is preserved during its propagation. In polarization channels, coupling between two orthogonally polarized components is occurred due to the cross-phase modulation (XPM) (Agrawal, 2001). So in our simulations the polarization coupling is considered and we use the following coupled equations to solve optical envelope of signals in two PSPs:

$$\begin{aligned} \frac{\partial A_x}{\partial z} + \beta_{1x} \frac{\partial A_x}{\partial t} + \frac{j\beta_2}{2} \frac{\partial^2 A_x}{\partial t^2} + \frac{\alpha}{2} A_x &= j\gamma (|A_x|^2 + \frac{2}{3}|A_y|^2) A_x \\ \frac{\partial A_y}{\partial z} + \beta_{1y} \frac{\partial A_y}{\partial t} + \frac{j\beta_2}{2} \frac{\partial^2 A_y}{\partial t^2} + \frac{\alpha}{2} A_y &= j\gamma (|A_y|^2 + \frac{2}{3}|A_x|^2) A_y \end{aligned} \tag{4.21}$$

where A_x, A_y are x- and y- polarization components of the optical field envelope, respectively, β_{1x} and β_{1y} are the inverse group delays for two polarization models. The β_{1x} and β_{1y} are different because of the modal birefringence. Usually β_2 and γ are the same for both polarization components.

4.3 PMD Model

To model polarization mode dispersion, we follow the approach of (Masayuki Matsumoto and Hasegawa, 1997). The fiber is modeled as a randomly varying birefringent medium that is a cascade of many short fibers with constant birefringence. The short fibers have identical length z_h and identical magnitude of linear birefringence Δn. The nonlinear propagation in these short fibers is governed by (4.21) with

$$\beta_{1x} - \beta_{1y} = \frac{\Delta n}{c}. \tag{4.22}$$

The PMD parameter D_p and birefringence Δn are related by

$$D_p = \sqrt{\frac{8}{3\pi}} \left(\frac{\Delta n}{c} \right) \sqrt{z_h}, \tag{4.23}$$

where c is the speed of light in free space. At fictitious junctions between fiber pieces, random axial rotation and addition of random phase difference between the two field components is incorporated by multiplying the vector field envelope by a matrix

$$M_{\theta,\varphi} = \begin{bmatrix} cos\theta & sin\theta e^{j\varphi} \\ -sin\theta e^{-j\varphi} & cos\theta \end{bmatrix}, \tag{4.24}$$

where θ and φ are uniformly distributed in the range of 0 to 2π and, from 0 to π, respectively. With this multiplication, the state of polarization (SOP) is made to traverse over all the points on the Poincaré sphere.

Chapter 5

System Setup and Simulation Results

Our evaluation on the DPolSK system are based on the BER performance in presence of noise, linear and nonlinear impairments. We conduct Monte-Carlo simulations to calculate the BER, a pseudo-random bit sequence (PRBS) of length $2^{16}-1$ is used in the simulations and the BER ranges from 1×10^{-4} to 1×10^{-1}. In this chapter, we simulate the photonic and opto-electronic components such as optical fibers, filters, erbium-doped fibre amplifier (EDFA), photodiodes, and evaluate the system performance. Then the main simulation results will be showed by comparing DPolSK with DPSK system.

5.1 Optical Fiber Communication System

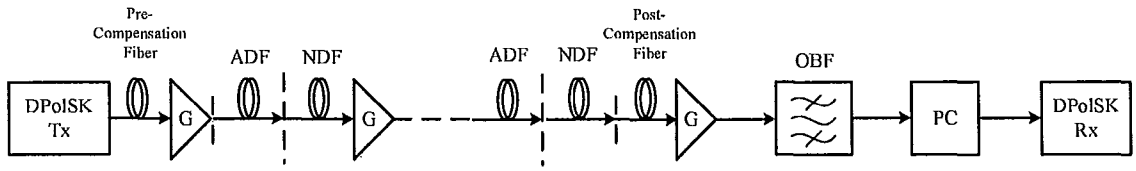

Figure 5.1: Schematic of optical communication system. NDF = Normal dispersion fiber, ADF = Anomalous dispersion fiber, OBF = Optical bandpass filter, PC = Polarization controller.

Fiber type	D (ps/nm/Km)	Length (Km)	$\gamma(W^{-1}Km^{-1})$
ADF	+17	40	1.1099
NDF	-14.5	40	1.1099
Pre-Comp (DCF)	-100	100	4.4
Pro-Comp (DCF)	-100	100	4.4

Table 5.1: The Parameters Used in the Simulations

As shown in Figure 5.1, a typical optical fiber transmission system includes transmitters, optical fibers, amplifiers, filters, and receivers. Our transmission system are consist of pre-compensation fiber, periodically placed dispersion-managed fiber, optical amplifier and post-compensation fiber. The dispersion-managed fiber is placed between amplifiers and it consist of a 40 Km long anomalous dispersion fiber (ADF) followed by a 40 Km long normal dispersion fiber (NDF). Chromatic Dispersion (CD) in modern optical fiber communication system can be easily compensated by dispersion-compensating fiber (DCF). In our simulations we have the pre-compensating fiber and pro-compensating fiber to compensate the remainder CD of fiber-optic systems. The fiber parameters in our simulations are listed in Table5.1.

5.1.1 Transmitter

Mach-zehnder modulators (MZM) are used to generate optical Gaussian pulses, under proper biasing conditions, the input signal can be represented as

$$\boldsymbol{E}_{in}(t) = \sum_{n} \boldsymbol{I}_n exp\left(-\frac{(t - nT_b - \frac{T_b}{2})^2}{T_0^2}\right), \tag{5.1}$$

where

$$\boldsymbol{I}_n = \begin{bmatrix} A_x \\ 0 \end{bmatrix} \tag{5.2}$$

for DPSK, and

$$\boldsymbol{I}_n = \begin{bmatrix} A_x \\ A_y \end{bmatrix} \tag{5.3}$$

for DPolSK, with $A_{x,y} \in \{e^{j0}, e^{j\pi}\}$. T_b is the bit period, in our simulations we have the bit rate 40 Gb/s so the bit period T_b is 25 ps. T_0 is the half-width of transmission Gaussian pulse at $1/e$-intensity point.The return-to-zero (RZ) pulse for OOK and DPSK is proved to have more tolerance to both linear and nonlinear impairments than non-return-to-zero (NRZ) format pulse (Wang and Kahn, 2004). In our simulations, we use the RZ format pulse and the duty cycle is 32%.

5.1.2 Optical Amplifier

Optical amplifier is used in each span of the fiber transmission to compensate the power loss. When the amplifier optical gain G is high enough, the principle source of noise in optical amplifier is amplified spontaneous emission (ASE). So in our amplifier simulation model, thermal noise and shot noise are ignored and only ASE noise is

taken into account. The ASE noise is given as a two-sided additive white Gaussian noise (AWGN) complex form in each polarization, with power spectral density (PSD) in each polarization given by

$$\rho_{ASE} = n_{sp}(G-1)h\nu \tag{5.4}$$

where n_{sp} is the spontaneous emission parameter and G is the amplifier gain, h is Planck's constant and ν is the optical carrier frequency. In our simulations we set $n_{sp} = 1.5$ and the bandwidth of ASE noise spectrum is 640 GHZ which is the same as sampling rate.

5.1.3 Optical Filter

An optical filter before the receiver is used to reduce the white background noise. The optimal optical filter is the matched filer when we assume the bandwidth of receiver filter is larger than that of optical filter (Ho, 2009). So the optimal filter for the Gaussian modulated pulse is also Gaussian. The transfer function of the optical matched filter for Gaussian pulse is given as

$$H(f) = exp\left(-\frac{f^2}{2f_0^2}\right), f_0 = \frac{1}{2\pi T_0} \tag{5.5}$$

where T_0 is the half-width of transmission Gaussian pulse at $1/e$-intensity point.

For the 32% RZ Gaussian pulse with 40 Gb/s bit rate, the optical matched Gaussian filter has a bandwidth of 280 GHZ.

5.2 Numerical Method

The NLSE equations (4.20) and (4.21) have no analytical solution and numerical method is needed to find the field at the end of the fiber-optic link. The most extensive numerical method that has been used for the pulse propagation equation is split-step Fourier method. The equation (4.21) can be rewritten as:

$$\begin{aligned} \frac{\partial A_x}{\partial z} &= (\hat{D}_x + \hat{N}_x)A_x \\ \frac{\partial A_y}{\partial z} &= (\hat{D}_y + \hat{N}_y)A_y \end{aligned} \tag{5.6}$$

where $\hat{D}_x$ and $\hat{D}_y$ are differential operators that account for linear effects containing dispersion and absorption. $\hat{N}_x$ and $\hat{N}_x$ are nonlinear operators representing effects caused by fiber nonlinearity. The operators are given by

$$\begin{aligned} \hat{D}_x &= -\beta_{1x}\frac{\partial}{\partial t} - \frac{j\beta_2}{2}\frac{\partial^2}{\partial t^2} - \frac{\alpha}{2} \\ \hat{D}_y &= -\beta_{1y}\frac{\partial}{\partial t} - \frac{j\beta_2}{2}\frac{\partial^2}{\partial t^2} - \frac{\alpha}{2} \end{aligned} \tag{5.7}$$

and

$$\begin{aligned} \hat{N}_x &= j\gamma(|A_x|^2 + \frac{2}{3}|A_y|^2) \\ \hat{N}_y &= j\gamma(|A_y|^2 + \frac{2}{3}|A_x|^2) \end{aligned} \tag{5.8}$$

Mathematically, we separate the linear and nonlinear operations and use the iterative equation as below

$$A_l(z+h,t) \approx \exp\left(\frac{h}{2}\hat{D}_l\right) exp\left(\int_z^{z+h} \hat{N}_l(z')dz'\right) exp\left(\frac{h}{2}\hat{D}_l\right) A_l(z,t)$$
$$\approx exp\left(\frac{h}{2}\hat{D}_l\right) [\hat{N}_l(z)h] exp\left(\frac{h}{2}\hat{D}_l\right) A_l(z,t), \qquad (5.9)$$

where $l = x, y$. The operator $exp\left(\frac{h}{2}\hat{D}\right)$ can be evaluated using fast fourier transform (FFT) (Agrawal, 2001).

5.3 Simulation Results

After setting up the system models, we conduct Monte-Carlo simulations to calculate BER in presence of linear and nonlinear impairments for DPolSK and DPSK systems.

5.3.1 Linear Performance

Figure 5.2 shows the BER as a function of fiber peak launch power for various modulation formats. To compare the optimum attainable performance using each of these formats, we have assumed that channel is ideal (no dispersion, no PMD and no nonlinearity). Fibers are modeled as loss elements and amplifiers compensate for loss exactly and add ASE. From Figure 5.2, we see that binary phase-shift keying (BPSK) has the best performance and polarization-shift keying (PolSK) is the worst. DPSK

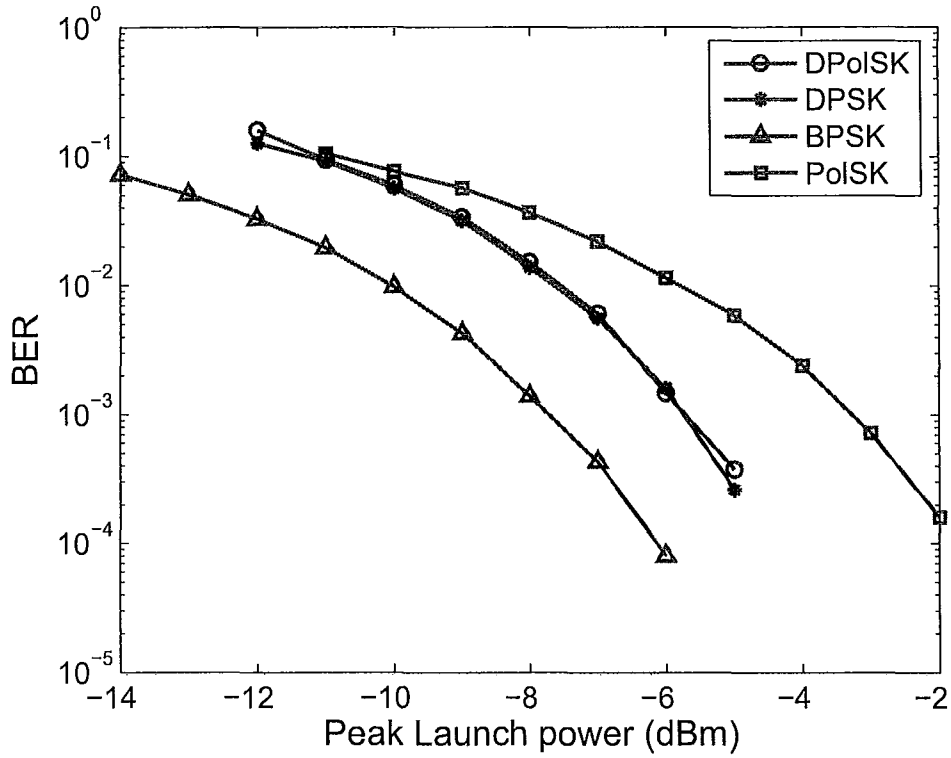

Figure 5.2: Linear BER performance of direct detection DPSK and DPolSK, coherent BPSK and PolSK. Transmission distance = 3200 Km

and DPolSK have roughly the same performance.

5.3.2 PMD Impairment

The PMD tolerance is studied extensively because it is considered as one of the critical obstacles for high-speed long-haul direct detection optical communication systems. Figure 5.3 shows the BER as a function of differential group delay (DGD) for DPolSK and DPSK. In our simulations, we choose a fiber length of 1600 Km and fixed the launch power at -8 dBm. We change the PMD parameter D_p from 0 to

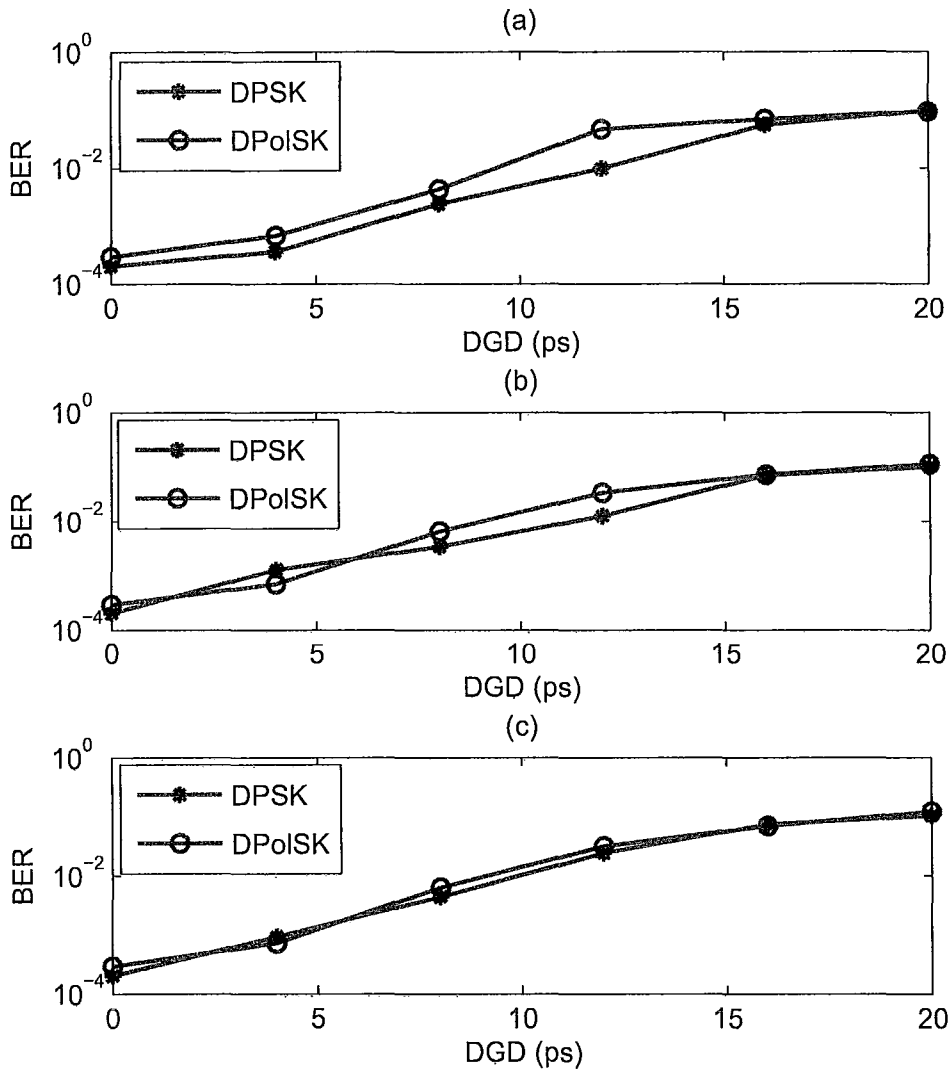

Figure 5.3: BER vs. DGD for DPolSK and DPSK systems. Transmission distance = 1600 Km and launch power = -8 dBm. Fiber dispersion and nonlinearity are set to zero. (a): 20 runs; (b): 40 runs; (c): 60 runs.

0.5 $ps/\sqrt{Km}$ with step size of 0.1 $ps/\sqrt{Km}$ and perform multiple runs by changing θ and φ and get the averaged value for each point. We perform 20, 40 and 60 runs and list the results as (a), (b), and (c), respectively in Figure 5.3. We can clearly see the trend that the DPSK and DPolSK curve get closer and closer as the calculations are increased. Since DPolSK is inherently polarization dependent, one might expect DPolSK has lower tolerance to PMD than DPSK. However, we see that DPolSK system has roughly the same PMD tolerance as DPSK system.

5.3.3 Fiber Nonlinearity and Dispersion

Fiber nonlinearity leads to impairments on the transmission system by causing spectrum broadening and noise amplification. In this subsection, we use the fiber parameters listed in Table5.1, ignore PMD and carry out the numerical simulations of DPSK and DPolSK systems. BER performance simulation results are shown in Figure 5.4. As can be seen, BER decreases initially with launch power. However, further increase in launch power, BER increases because of the fiber nonlinear effects causing performance degradation. DPolSK has higher nonlinear tolerance than DPSK systems and therefore, it gives better performance when the launch power is optimized. DPSK has been found to have higher nonlinear tolerance than OOK and BPSK (Ho, 2003a) because of the differential detection which leads to partial cancellation of intra-channel cross-phase modulation (IXPM). We believe that the DPolSK has higher nonlinear tolerance because of differential detection. The performance advantage of DPolSK over DPSK can be understood as follows. In the case of DPSK, the phases of the neighboring symbols vary, but the polarization angles are roughly the same. However,

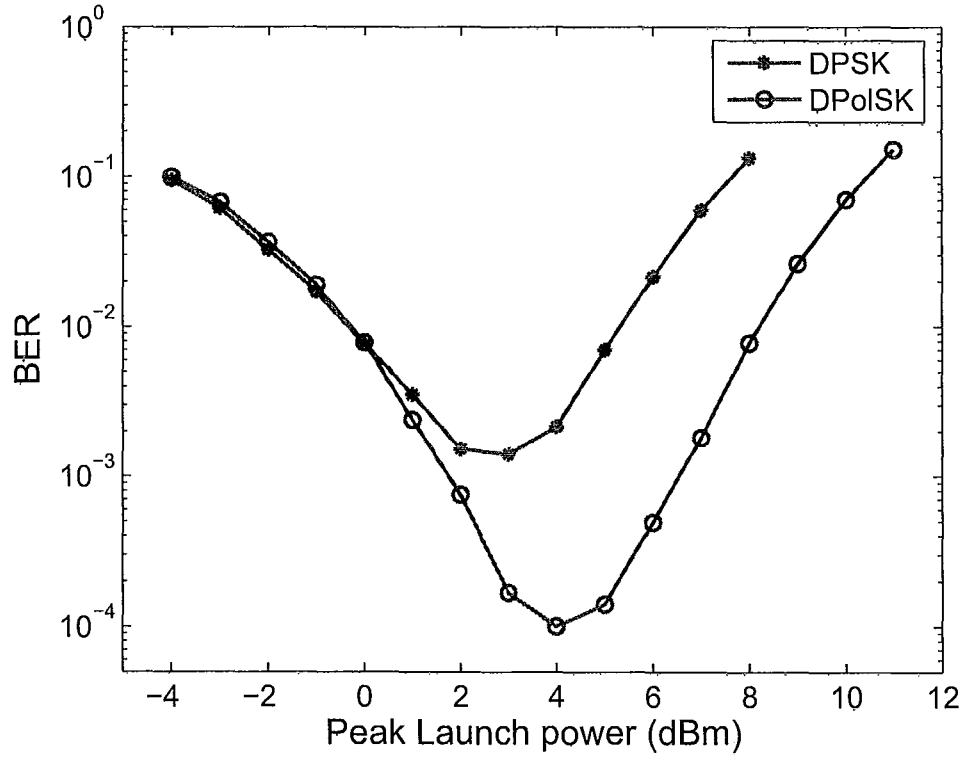

Figure 5.4: BER vs. peak launch power for DPSK and DPolSK systems. Transmission distance = 16000 Km. PMD is ignored.

for DPolSK signals, there is a $\pi/2$ polarization rotation between adjunct symbols and therefore, the phases as well as polarization angles of the neighboring symbols vary and thereby, a better averaging of IFWM is achieved. In other words, the generation of ghost pulses due to IFWM is not very efficient in DPolSK systems as compared to DPSK systems, leading to higher nonlinear tolerance.

To confirm this fact, we have simulated the propagation of 3 signal pulses with a bit sequence '00' and '11'. The initial symbol is

$$\boldsymbol{E}_1 = \begin{bmatrix} A \\ 0 \end{bmatrix}. \tag{5.10}$$

For DPSK, the symbol sequence corresponding to '00' is

$$\begin{bmatrix} A \\ 0 \end{bmatrix} \begin{bmatrix} -A \\ 0 \end{bmatrix} \begin{bmatrix} A \\ 0 \end{bmatrix}. \tag{5.11}$$

For DPolSK, the corresponding symbol sequence is

$$\begin{bmatrix} A \\ 0 \end{bmatrix} \begin{bmatrix} 0 \\ A \end{bmatrix} \begin{bmatrix} -A \\ 0 \end{bmatrix}. \tag{5.12}$$

Similarly, when bit sequence '11' is sent, the symbol sequence for DPSK is

$$\begin{bmatrix} A \\ 0 \end{bmatrix} \begin{bmatrix} A \\ 0 \end{bmatrix} \begin{bmatrix} A \\ 0 \end{bmatrix}, \tag{5.13}$$

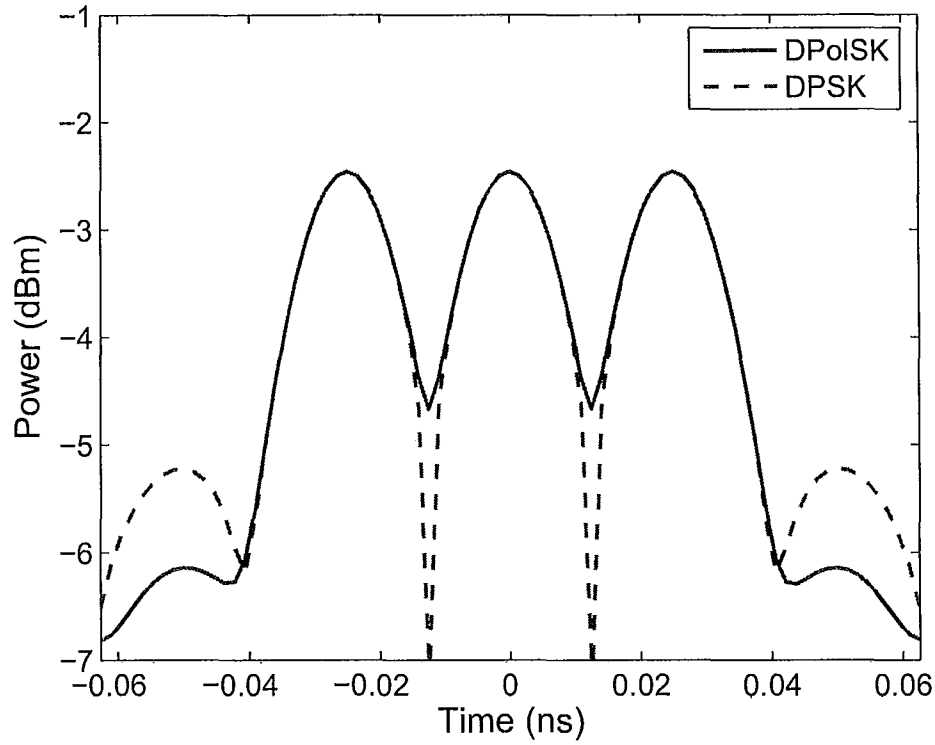

Figure 5.5: Ghost pulse generation in DPolSK and DPSK systems. Bit sequence '00' is sent, fiber length = 16000 Km, peak launch power = 6 dBm, ASE noise and PMD are turned off.

and the symbol sequence for DPolSK is

$$\begin{bmatrix} A \\ 0 \end{bmatrix} \begin{bmatrix} 0 \\ -A \end{bmatrix} \begin{bmatrix} -A \\ 0 \end{bmatrix}. \tag{5.14}$$

Because of fiber dispersion, the pulses spread and the nonlinear interaction among the pulses leads to ghost pulses on either side of the signal pulses (Mamyshev and Mamysheva, 1999), (R. J. Essiambre and Raybon, 1999), (Shiva Kumar and Chowdhury, 2002). If the signal pulses are present in these symbol slots, ghost pulses would interfere with them leading to nonlinear signal distortions. Figure 5.5 and 5.6 show

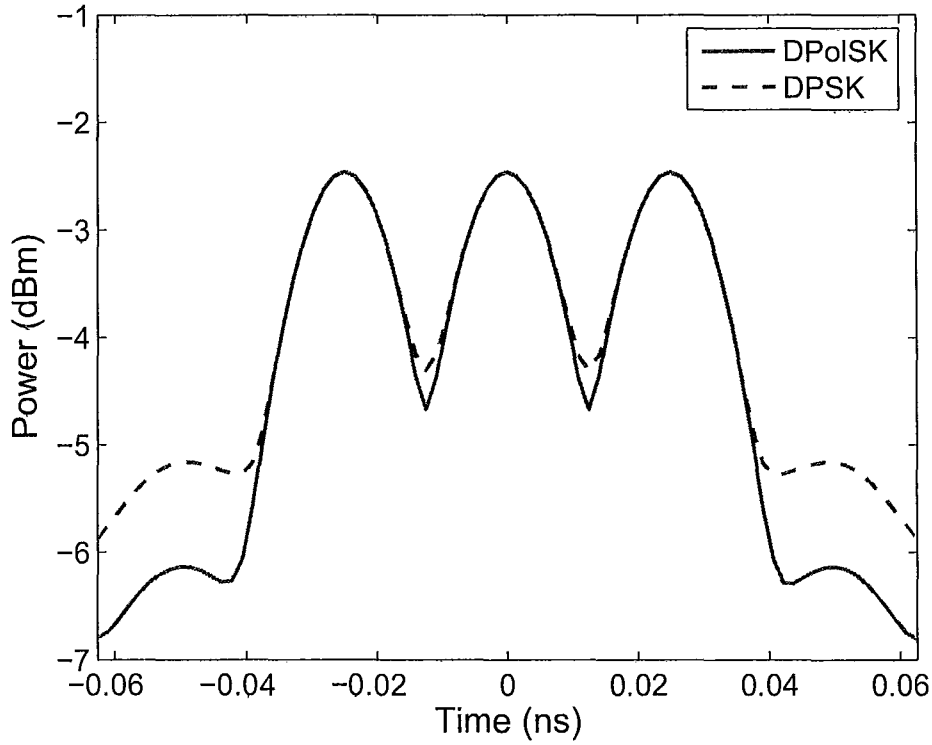

Figure 5.6: Ghost pulse generation in DPolSK and DPSK systems. Bit sequence '11' is sent, fiber length = 16000 Km, peak launch power = 6 dBm, ASE noise and PMD are turned off.

the signal and ghost pulses at the end of the fiber-optic link for systems based on DPSK and DPolSK when bit sequence '00' and '11' are sent, respectively. As can be seen from both figures, the ghost pulses are significantly suppressed in the case of DPolSK as compared to DPSK.

5.3.4 PMD, Dispersion, and PMD

In a realistic optical communication system, both of the fiber nonlinearity and PMD are two critical impairments for the system. We have simulated the BER

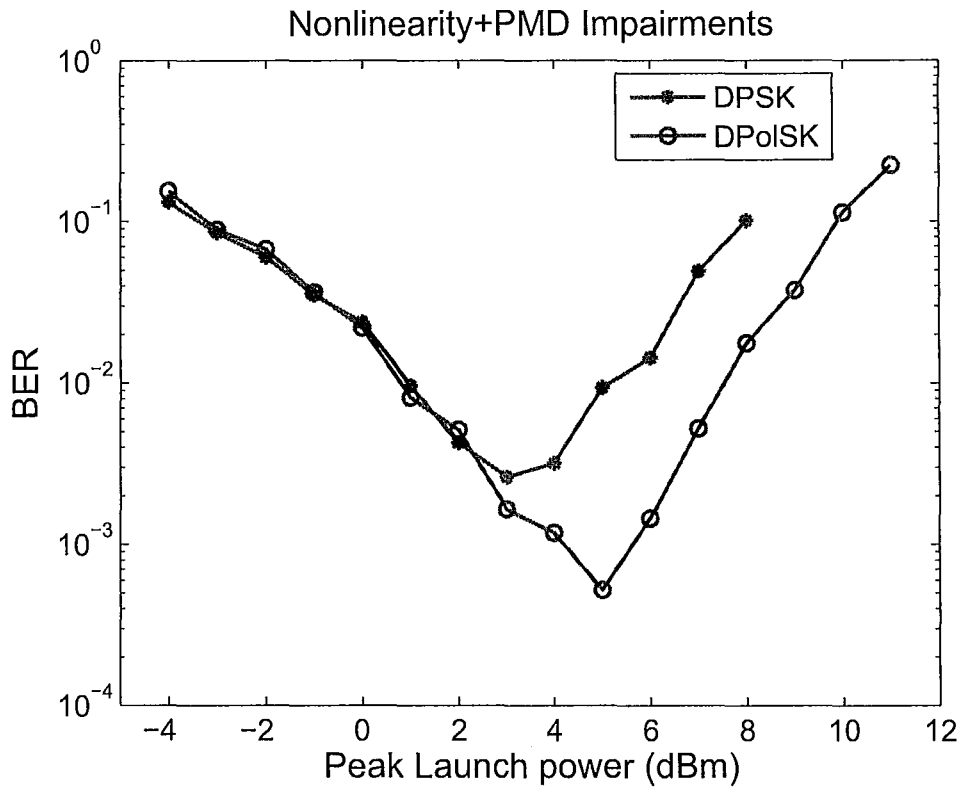

Figure 5.7: BER vs. peak launch power. Transmission distance = 16000 Km, PMD parameter $D_p = 0.05\ ps/\sqrt{Km}$

performance of DPSK and DPolSK systems with both nonlinearity and PMD included in figure 5.7. We choose the nonlinear parameter γ which is the same as the previous simulation and the PMD parameter D_p as 0.05 $ps/\sqrt{Km}$. In the simulations, the fiber length is 16000 Km, and 25 runs are conducted and averaged for each point of of the BER curves.

Comparing figures 5.4 and 5.7, we see that the performance of DPolSK system is degraded slightly due to PMD. Nevertheless, the system based on DPolSK is superior to DPSK in the presence of nonlinearity and PMD.

Chapter 6

Conclusions

We propose a novel differential polarization-shift keying (DPolSK) system in this thesis. To transmit a bit '1' ('0'), the polarization angle of the current symbol is shifted by $\pi/2$ $(-\pi/2)$ with respect to the previous symbol. A novel balanced detector consisting of optical delay interferometer and Faraday rotator to demodulate the DPolSK signals is also proposed. Monte-carlo simulations are conducted to evaluate BER performances of the DPolSK system as well as DPSK system in the presence of chromatic dispersion (CD), polarization mode dispersion (PMD) and fiber nonlinearity (FNL).

Since the DPolSK is sensitive to polarization variations during the transmission, our simulation system is setup based on a polarization channel and channel fluctuations such as polarization and phase angle variations are considered. To minimize the polarization variations effect on DPolSK system, a polarization controller (PC) is used to maximize the receiver current.

Without dispersion and nonlinearity, the linear simulation results show DPolSK

system has the same bit-error-rate (BER) performance with DPSK system. These results validate the theoretical BER analysis about the two systems in the presence of additive white Gaussian noise (AWGN). The BER performances in presence of PMD also show DPolSK system has the same tolerance to PMD as DPSK system.

The advantage of DPolSK system over DPSK is that DPolSK has higher nonlinear tolerance. The simulation results show the ghost pulse generation induced by intra-channel four-wave mixing (IFWM) is significantly suppressed in the case of DPolSK as compared to DPSK. The reason for DPolSK nonlinear tolerance advantage can be explained as follows. In the case of DPSK, the phases of the neighboring symbols vary, but the polarization angles are roughly the same. However, for DPolSK signals, there is a $\pi/2$ polarization rotation between adjunct symbols and therefore, the phases as well as polarization angles of the neighboring symbols vary and thereby, a better averaging of IFWM is achieved. In other words, the generation of ghost pulses due to IFWM is not very efficient in DPolSK systems as compared to DPSK systems, leading to higher nonlinear tolerance.

Finally, there are still some work we can go into in the future. Because our evaluation of the DPolSK system is based on the single-channel, so the next step is to study the new DPolSK scheme in wavelength division multiplexing (WDM) systems. The impact of inter-channel nonlinear effects on DPolSK system will be found and compared with other modulation schemes.

Bibliography

Agrawal, G. P. (2001). *Nonlinear Fiber Optics.*

Benedetto, S. and Poggiolini, P. (1992). Theory of polarization shift keying modulation. *IEEE Trans. Commun.*, **40**, 708–721.

Chongjin Xie, Lothar Moller, H. H. and Hunsche, S. (2003). Comparison of System Tolerance to Polarization-Mode Dispersion Between Different Modulation Formats. *IEEE Photon. Technol. Lett.*, **15**, 1168–1170.

Chris Xu, Xiang Liu, a. X. W. (2004). Differential Phase-Shift Keying for High Spectral Efficiency Optical Transmissions. *IEEE J. Sel. Topics Quantum Electron.*, **10**, 281–293.

Dany-Sebastien Ly-Gagnon, Satoshi Tsukamoto, K. K. a. K. K. (2006). Coherent Detection of Optical Quadrature Phase-Shift Keying Signals With Carrier Phase Estimation. *IEEE J. Lightwave Technol.*, **24**, 12–21.

Gnauck, A. H. and Winzer, P. J. (2005). Optical Phase-Shift-Keyed Transmission. *IEEE J. Lightwave Technol.*, **23**, 115–130.

Gnauck, A. H., R. G. C. S. L. J. D. C. S. L. A. A. B. S. G. D. H. S. K. A. M. A. M. D. M. M. L. X. X. C. W. X. and Gill, D. M. (2002). 2.5 Tb/s (64 x

42.7 Gb/s)transmission over 40 x 100 km NZDSF using RZ-DPSK format and all-Raman-amplified spans. *Optical Fiber Commun. Conf.*

Godard, D. N. (1980). Self-Recovering Equalization and Carrier Tracking in Two-Dimensional Data Communication Systems. *IEEE Trans. Commun.*, **28**, 1867–1875.

Goldfarb, G. and Li, G. (2006). BER estimation of QPSK homodyne detection with carrier phase estimation using digital signal processing. *Opt. Express*, **14**, 8043–8053.

Gordon, J. P. and Mollenauer, L. F. (1990). Phase noise in photonic communications systems using linear amplifiers. *Opt. Lett.*, **15**, 1351–1353.

Griffin, R. A. and Carter, A. C. (2002). Optical differential quadrature phase-shift key (oDQPSK) for high capacity optical transmission. *Tech. Dig. OFC*, pages 367–368.

Han, Y. and Li, G. (2004). Direct detection differential polarization-phase-shift keying based on Jones vector. *Opt. Express*, **12**, 5821–5826.

Han, Y. and Li, G. (2005). Coherent optical communication using polarization multiple-input-multiple-output. *Opt. Express*, **13**, 7527–7534.

Ho, K.-P. (2003a). Performance Degradation of Phase-Modulated Systems due to Nonlinear Phase Noise. *IEEE J. Photon. Technol Lett.*, **15**, 1213–1215.

Ho, K.-P. (2003b). Performance degradation of phase-modulated systems with nonlinear phase noise. *IEEE Photon. Technol. Lett.*, **15**, 1213–1215.

Ho, K.-P. (2005). *Phase-Modulated Optical Communications.*

Ho, K.-P. (2009). Optimal optical filter for a short pulse with a bandwidth-limited receiver. *Opt. Lett.*, **34**, 932–934.

Hou, K.-S. and Wu, J. (2002). A Differential Coding Method for the Symmetrically Differential Polarization Shift-Keying System. *IEEE Trans. Commun.*, **50**, 2042–2051.

Humblet, P. A. and Azizoglu, M. (1991). On the bit error rate of lightwave systems with optical amplifiers. *IEEE J. Lightwave Technol.*, **9**, 1576–1582.

Jaume Comellas, J. M. G. and Prat, J. (2004). Quaternary Optical Transmission System Combining Phase and Polarization-Shift Keying. *IEEE Photon. Technol. Lett.*, **16**, 1766–1768.

Kikuchi, K. (2006). Phase-diversity homodyne detection of multilevel optical modulation with digital carrier phase estimation. *IEEE J. Sel. Quantum Electron.*, **12**, 563–570.

Kim, H. and Gnauck, A. H. (2003). Experimental investigation of the performance limitation of DPSK systems due to nonlinear phase noise. *IEEE Photon. Technol. Lett.*, **15**, 320–322.

Li, G. (2009). Recent advances in coherent optical communication. *Advances in Optics and Photonics*, **1**, 279–307.

Mamyshev, P. V. and Mamysheva, N. A. (1999). Pulse-overlapped dispersion-managed data transmission and intrachannel four-wave mixing. *Opt. Lett.*, **24**, 1454–1456.

Masayuki Matsumoto, Y. A. and Hasegawa, A. (1997). Propagation of solitons in fibers with randomly varying birefringence: effects of soliton transmission control. *IEEE J. Lightwave Technol.*, **15**, 584–589.

Misha Boroditsky, Misha Brodsky, N. J. F. P. M. C. A. and Mecozzi, A. (2005). Outage Probabilities for Fiber Routes With Finite Number of Degrees of Freedom. *IEEE Photon. Technol. Lett.*, **17**, 345–347.

R. J. Essiambre, B. M. and Raybon, G. (1999). Intra-channel cross-phase modulation and four-wave mixing in high-speed TDM systems. *Electron. Lett.*, **35**, 1576–1578.

S. Benedetto, R. G. and Poggiolini, P. (1995). Direct Detection of Optical Digital Transmission Based on Polarization Shift Keying Modulation. *IEEE J. on Sel. Areas Commun.*, **13**, 531–542.

Shiva Kumar, John C. Mauro, S. R. and Chowdhury, D. Q. (2002). Performance Degradation of Phase-Modulated Systems due to Nonlinear Phase Noise. *IEEE J. Sel. Quantum Electron.*, **8**, 626–631.

W. Christoph, L. J. and R.Werner (2002). RZ-DQPSK format with high spectral efficiency and high robustness toward fiber nonlinearities. *ECOC, Copenhagen, Denmark.*

Wang, J. and Kahn, J. M. (2004). Impact of Chromatic and Polarization-Mode Dispersions on DPSK Systems Using Interferometric Demodulation and Direct Detection. *IEEE J. Lightwave Technol.*, **22**, 362–371.

Winzer, P. J. and Essiambre, R.-J. (2006). Advanced modulation formats for high-capacity optical transport networks. *IEEE J. Lightwave Technol.*, **24**, 4711–4728.

Winzer, P. J. and Essiambre, R.-J. (2008). Advanced optical modulation formats. *Optical Fiber Telecommunications V B: systems and networks*, **1**, 23–92.

You Imai, K. I. and James, R. T. B. (1990). Phase-Noise-Free Coherent Optical Communication System Utilizing Differential Polarization Shift Keying (DPolSK). *IEEE J. Lightwave Technol.*, **5**, 691–698.

Yutaka Miyamoto, Akira Hirano, S. K. M. T. a. Y. T. (2002). Novel modulation and detection for bandwidth-reduced RZ formats using duobinary-mode splitting in wideband PSK/ASK conversion. *IEEE J. Lightwave Technol.*, **20**, 2067–2078.